The Journal of Immunology

Rapid Turnover and High Production Rate of Myeloid Cells in Adult Rhesus Macaques with Compensations during Aging

Ziyuan He, Carolina Allers, Chie Sugimoto, Nursarat Ahmed, Hideki Fujioka, Woong-Ki Kim, Elizabeth S. Didier and Marcelo J. Kuroda

J Immunol 2018; 200:4059-4067; Prepublished online 4 May 2018;
doi: 10.4049/jimmunol.1800207
http://www.jimmunol.org/content/200/12/4059

The Journal of Immunology is published twice each month by
The American Association of Immunologists, Inc.,
1451 Rockville Pike, Suite 650, Rockville, MD 20852

Print ISSN: 0022-1767 Online ISSN: 1550-6606.

Rapid Turnover and High Production Rate of Myeloid Cells in Adult Rhesus Macaques with Compensations during Aging

Ziyuan He,*,† Carolina Allers,* Chie Sugimoto,*,[1] Nursarat Ahmed,* Hideki Fujioka,‡ Woong-Ki Kim,§ Elizabeth S. Didier,¶ and Marcelo J. Kuroda*,†

Neutrophils, basophils, and monocytes are continuously produced in bone marrow via myelopoiesis, circulate in blood, and are eventually removed from circulation to maintain homeostasis. To quantitate the kinetics of myeloid cell movement during homeostasis, we applied 5-bromo-2′-deoxyuridine pulse labeling in healthy rhesus macaques (*Macaca mulatta*) followed by hematology and flow cytometry analyses. Results were applied to a mathematical model, and the blood circulating half-life and daily production, respectively, of each cell type from macaques aged 5–10 y old were calculated for neutrophils (1.63 ± 0.16 d, 1.42 × 10^9 cells/l/d), basophils (1.78 ± 0.30 d, 5.89 × 10^6 cells/l/d), and $CD14^+CD16^-$ classical monocytes (1.01 ± 0.15 d, 3.09 × 10^8 cells/l/d). Classical monocytes were released into the blood circulation as early as 1 d after dividing, whereas neutrophils remained in bone marrow 4–5 d before being released. Among granulocytes, neutrophils and basophils exhibited distinct kinetics in bone marrow maturation time and blood circulation. With increasing chronological age, there was a significant decrease in daily production of neutrophils and basophils, but the half-life of these granulocytes remained unchanged between 3 and 19 y of age. In contrast, daily production of classical monocytes remained stable through 19 y of age but exhibited a significant decline in half-life. These results demonstrated relatively short half-lives and continuous replenishment of neutrophils, basophils, and classical monocytes during homeostasis in adult rhesus macaques with compensations observed during increasing chronological age. ***The Journal of Immunology*****, 2018, 200: 4059–4067.**

Granulocytes (including neutrophils, eosinophils, and basophils) and monocytes are myeloid-lineage cells that differentiate from myeloblasts in bone marrow and are well known for participation in innate immune responses for pathogen clearance and inflammation. Their production in bone marrow, circulation kinetics, and subsequent removal are tightly regulated to maintain homeostasis (1, 2). Qualitative descriptions of myeloid cell development and regulatory mechanisms have been reported, but quantitative measures such as half-life and production rate in vivo are less clearly understood (3, 4).

During homeostasis, myeloid cells are continuously produced via bone marrow hematopoiesis. Precursor cells are generated from hematopoietic stem cells (HSCs) and retained in bone marrow while undergoing differentiation. Neutrophils are the predominant WBC population, ranging from 20 to 50% in rhesus macaques. Mature neutrophils leave bone marrow, enter and circulate in blood, and then leave circulation after a specified period of time (3). In contrast, basophils compose <1% of WBC during homeostasis, although their numbers may increase during parasite infections and allergic inflammation (5, 6). Little is known about basophil development and kinetics during homeostasis, mainly due to their scarcity at steady state. Monocytes compose between 2 and 10% of WBC. At least three subsets have been identified in humans and rhesus macaques, consisting of $CD14^+/CD16^-$ classical monocytes, $CD14^+/CD16^+$ intermediate monocytes, and $CD14^-/CD16^+$ nonclassical monocytes; these subsets exhibit distinctive kinetics (7, 8).

Limitations exist for defining the half-life of myeloid cells in humans due to potential toxicity of in vivo labels and difficulty in consecutive bone marrow and blood sampling needed to validate cell kinetics. Translating results from rodents is confounded by the more predominant lymphocytes in mouse blood compared with the higher percent of neutrophils in human blood (9, 10). Thus, nonhuman primates are relevant because they are genetically and physiologically similar to humans, exhibit a similar WBC composition as humans, and can be applied to more effective in vivo cell proliferation labeling and specimen sampling. The purpose of this study, therefore, was to 1) develop a mathematical model to investigate and compare the kinetics of neutrophils, basophils, and classical monocytes in adult rhesus macaques using in vivo pulse 5-bromo-2′-deoxyuridine (BrdU) labeling, 2) confirm the biological relevance of the model by sampling bone marrow after the administration of the label, and 3) apply the model to a cohort of older animals to investigate the chronological aging effects on the kinetics of myeloid cells.

*Division of Immunology, Tulane National Primate Research Center, Tulane University Health Science Center, Covington, LA 70433; †Department of Microbiology and Immunology, Tulane University School of Medicine, New Orleans, LA 70112; ‡Center for Computational Science, Tulane University, New Orleans, LA 70118; §Department of Microbiology and Molecular Cell Biology, Eastern Virginia Medical School, Norfolk, VA 23507; and ¶Division of Microbiology, Tulane National Primate Research Center, Tulane University Health Science Center, Covington, LA 70433

[1]Current address: Laboratory of International Epidemiology, Dokkyo Medical University, Tochigi, Japan.

ORCIDs: 0000-0003-3556-8248 (Z.H.); 0000-0001-8576-770X (C.A.); 0000-0002-8343-7202 (E.S.D.).

Received for publication February 13, 2018. Accepted for publication April 10, 2018.

This work was supported by research funding from the National Institutes of Health (Grants AI097059 and AI110163 to M.J.K., MH108458 and MH107333 to W.-K.K., AG052349 to E.S.D., HL139278 to E.S.D. and M.J.K., and OD011104 to the Tulane National Primate Research Center). This study was also supported by Virginia's Commonwealth Health Research Board Grant 11-09 to W.-K.K.

Address correspondence and reprint requests to Dr. Marcelo J. Kuroda at the current address: Center for Comparative Medicine and California National Primate Research Center, University of California, Davis, County Road 98 and Hutchison Drive, Davis, CA 95616. E-mail address: mjkuroda@ucdavis.edu

The online version of this article contains supplemental material.

Abbreviations used in this article: BrdU, 5-bromo-2′-deoxyuridine; FSC, forward scatter; HSC, hematopoietic stem cell; MPO, myeloperoxidase; SSC, side scatter.

Materials and Methods

Rhesus macaques

Forty-five Indian-origin rhesus macaques, specific pathogen-free for SIV, Type D Simian Retrovirus, and Simian T cell Leukemia Virus type 1 from the Tulane National Primate Research Center were studied (Table I). One group comprised 11 adult males between 5 and 10 y of age to study myeloid cell kinetics. A second group of 33 males and females ranging from 3 to 20 y of age were used to consider the effects of chronological aging on myeloid cell kinetics. All procedures were in accordance with the *National Institutes of Health Guide for the Care and Use of Laboratory Animals* and approved by the Tulane University Institutional Animal Care and Use Committee (11).

BrdU administration and collection of blood and bone marrow specimens

BrdU (B5002-100G; Sigma-Aldrich), a thymidine analog, was prepared at 30 mg/ml in endotoxin-free PBS (TMS-012-A; EMD Millipore), filter-sterilized through 0.2-μm polyethersulfone membranes (Steriflip, SCGP00525 or 09-740-2A; Fisher Scientific), and administered i.v. at a dose of 60 mg/kg body weight. Blood and bone marrow aspirates were obtained between 8 AM and 11 AM on collection days after BrdU injections to minimize effects of daily oscillations on the kinetics studies.

Flow cytometry and hematology analyses

Cellular immunophenotyping and staining for BrdU incorporation were performed as described (8, 12). Briefly, 200 μl of EDTA-anticoagulated whole blood was washed and stained with surface mAb mixtures (Table II). RBCs were lysed with FACS lysing solution (BD Biosciences, San Jose, CA), and remaining cells were permeabilized with a three-step Cytofix/Cytoperm protocol per the manufacturer's instructions (BD Biosciences). Bone marrow aspirates were washed, filtered through a 100-μm cell strainer (Corning, Corning, NY), and treated with 10 ml of ammonium-chloride-potassium lysing buffer (ACK Lysing Buffer; Lonza) to remove RBCs. Approximately one million bone marrow cells were then stained the same way as for whole blood. Samples were acquired with a LSR II or LSRFortessa flow cytometer (BD Biosciences) and data were analyzed with FlowJo software (version 10; FlowJo, Ashland, OR). Hematology analyses were performed on a Sysmex XT-2000iV automated hematology analyzer (Sysmex America, Lincolnshire, IL). Absolute cell counts for neutrophils and basophils were directly measured from the automated hematology analyzer. The absolute cell counts for classical monocytes were calculated from the percentages of classical monocytes in the overall monocyte population (including classical monocytes, intermediate monocytes, and nonclassical monocytes) by flow cytometry analysis and multiplied by the absolute cell counts for all monocytes.

Mathematical modeling

We developed a mathematical model applying the BrdU incorporation kinetics data to estimate the turnover rates and half-lives of each myeloid cell population. This was based on the following consensus assumptions of myeloid cell development. 1) Myeloid cells divide in bone marrow, enter blood circulation as G_0 phase (without further proliferation), and subsequently leave the blood circulation to enter tissues or undergo clearance. 2) BrdU is incorporated into dividing myeloid progenitor cells in bone marrow almost immediately after injection, and unincorporated BrdU decays relatively soon after injection (13, 14). 3) After division, BrdU-labeled precursor cells remain in the bone marrow for T days (defined as bone marrow transit time). 4) Only mature cells egress from bone marrow and enter the blood circulation in a one-phase decay rate. 5) During homeostasis, the numbers of each cell population in blood and precursor cell population in bone marrow remain stable. For example, it is assumed that neutrophils leave the blood circulation at the same rate that bone marrow mature neutrophils enter blood circulation to retain stable numbers during homeostasis.

We designated p as the proliferation production rate for each type of cells in bone marrow, N_m as the number of each type of mature myeloid cell (i.e., neutrophils, basophils, and classical monocytes) in bone marrow, k_1N_m as the rate at which mature cells from bone marrow enter blood circulation, N_b as the number of each type of labeled myeloid cell in blood, k_2N_b as the rate of each type of myeloid cell leaving blood circulation, and T as bone marrow transit time. Therefore, we calculated the kinetics of mature cells in bone marrow as

$$\frac{dN_m(t)}{dt} = p - k_1N_m(t) \tag{1}$$

in the blood because mature neutrophils enter after transit time T:

$$\frac{dN_b(t)}{dt} = k_1N_m(t-T) - k_2N_b(t) \tag{2}$$

During homeostasis, each type of cell numbers in blood remain stable (Assumption 5), which means $dN_b(t)/dt = 0$, so $k_1N_m = k_2N_b$.

We assumed labeled cells have the same kinetics as above. Because we used single-bolus injection of BrdU and the unincorporated BrdU was cleared quickly after injection (Assumption 2), dividing cells were labeled over a short time. Thus, we can ignore the proliferation input over time ($p = 0$). We then let L_m be the number of mature labeled cells in bone marrow, and L_b be the labeled cells in blood. Similarly, we calculated the kinetics of labeled cells as

$$\frac{dL_m(t)}{dt} = -k_1L_m(t) \tag{3}$$

$$\frac{dL_b(t)}{dt} = k_1L_m(t-T) - k_2L_b(t) \tag{4}$$

Dividing Eq. 3 and Eq. 4 by N_m and N_b, respectively, and using $k_1N_m = k_2N_b$,

$$\frac{dL_m(t)}{N_m dt} = -k_2\frac{N_b}{N_m}\frac{L_m(t)}{N_m} \tag{5}$$

$$\frac{dL_b(t)}{N_b dt} = k_2\frac{N_b}{N_m}\frac{L_m(t-T)}{N_b} - k_2\frac{L_b(t)}{N_b} \tag{6}$$

Let $M = L_m(t)/N_m$ be the ratio of labeled/total precursor cells in bone marrow, $B = L_b(t)/N_b$ be the ratio of labeled/total cells in blood, $k = k_2$, and $R = N_b/N_m$ assuming N_m and N_b are constant, then Eq. 5 and Eq. 6 transform to

$$\frac{dM(t)}{dt} = -kRM(t) \quad \text{for } t > 0 \tag{7}$$

$$\frac{dB}{dt} = kM(t-T) - kB(t) \quad \text{for } t > T \tag{8}$$

The solution of Eq. 7 is

$$M(t) = M_0 exp(-kRt) \tag{9}$$

where M_0 is M at $t = 0$. Assuming $B = 0$ at $t = T$, the solution of Eq. 8 for $t > T$ is

$$B(t) = \frac{M_0k}{k(R-1)}\{exp(kT) - exp[RkT - k(R-1)t]\}exp(-kt) \tag{10}$$

Applying Tayler series approximation around $t \sim T$ to the term,

$$exp[RkT - k(R-1)t] \cong exp(kT) - k(R-1)exp(kT)(t-T) + \ldots \tag{11}$$

Thus, the simplified expression is

$$B(t) = M_0k\,exp(kT)(t-T)exp(-kt) \tag{12}$$

which is

$$B(t) = M_0k(t-T)exp[-k(t-T)] \tag{13}$$

We fitted Eq. 13 to the blood BrdU kinetics data using the *scipy.optimize.curve_fit* function from the SciPy library for nonlinear least squares (15). Calculations were performed using IPython Notebook (Python version 2.7), and best-fit curves are shown in Supplemental Fig. 2C. Calculated parameters in Supplemental Table I are blood half-life = $\ln 2/k$, blood average lifespan = $1/k$, and daily production = absolute number of cells in blood / average lifespan of cells in blood.

Statistical analyses

Spearman correlation test was used to compare half-lives or daily productions in relation to ages of the monkeys. Kruskal–Wallis analyses were used to compare results between different age groups of monkeys. Graphs were prepared using GraphPad Prism (version 7; San Diego, CA), and $p < 0.05$ was considered significant.

Table I. Animals used in the study

Group 1			Group 2		
ID	Sex	Age (y)	ID	Sex	Age (y)
DG09	M	10.3	GP56	M	3.0
DR67	M	9.2	GM77	M	3.1
EM89	M	8.2	GL96	M	3.2
ER17	M	8.3	GH64	M	3.3
FI38	M	7.8	FG54	M	5.2
GK40	M	5.5	FF01	F	5.3
GN17	M	5.8	EM66	F	6.2
GN24	M	5.2	EL53	M	6.2
HA52	M	5.0	EF03	F	6.3
IR99	M	6.2	EM25	F	6.9
IT27	M	5.7	EE66	F	7.5
			DJ87	F	8.3
			DG85	F	8.3
			BR31	F	10.5
			BJ22	F	11.0
			BG19	F	11.4
			AM92	F	12.3
			AI70	F	12.4
			T053	M	14.4
			P306	M	16.3
			P153	M	16.3
			CN73	M	16.4
			HF74	F	17.8
			IR93	F	18.5
			IR86	F	18.9
			IR91	F	18.9
			HF73	F	19.0
			IR89	F	19.0
			IR87	F	19.4
			IR94	F	19.4
			IR85	F	19.4
			IR92	F	19.5
			IR88	F	19.5
			IR90	F	19.5

M, male; F, female.

Table II. Abs used in the study

Ab	Clone	Source
CD1c	AD5-8E7	Miltenyi Biotec
CD3	SP34-2	BD Biosciences
CD8	SK1	BD Biosciences
CD11b	ICRF44	BD Biosciences
CD11c	3.9	eBioscience
CD14	M5E2	BD Biosciences
CD16	3G8	BD Biosciences
CD20	B9E9	Beckman Coulter
CD45	MB4-6D6	Miltenyi Biotec
CD123	7G3	BD Biosciences
CD163	Mac2-158	Trillium
CD169	7-239	BioLegend
HLA-DR	L243	BD Biosciences
MPO	5B8	BD Biosciences
BrdU	3D4	BD Biosciences

Results

Phenotype analysis of neutrophils, basophils, and monocytes in blood of rhesus macaques

Healthy rhesus macaques (Table I) were administered a single i.v. bolus of BrdU (60 mg/kg body weight) to label dividing progenitor cells in bone marrow. Flow cytometry phenotyping (Abs listed in Table II) was used to identify neutrophil, basophil, and monocyte populations in blood of rhesus macaques (Fig. 1A). Granulocytes and monocytes were first gated from intermediate to high forward scatter (FSC) and side scatter (SSC) fractions and then separated based on the expression of HLA-DR. Granulocytes were $CD3^-/CD8^-/CD20^-/HLA\text{-}DR^-$ and monocytes/dendritic cells were $CD3^-/CD8^-/CD20^-/HLA\text{-}DR^+$. Within granulocytes, basophils stained brightly for CD123 expression, whereas neutrophils were negative for CD123. Interestingly, basophils in rhesus macaques appeared higher in the SSC region (Supplemental Fig. 1), whereas human basophils usually were in the lower SSC area with lymphocyte lineage populations under homeostatic conditions (16). This gating strategy for neutrophils was confirmed by expression of myeloperoxidase (MPO). As expected, MPO was detected at high levels in neutrophils and classical monocytes but not in lymphocytes and basophils (Fig. 1B).

Monocyte populations were gated as intermediate in FSC and SSC and for staining $CD3^-/CD8^-/CD20^-/HLA\text{-}DR^+$. From these nonlymphocytic $HLA\text{-}DR^+$ cells, monocyte subsets were separated as $CD14^+/CD16^-$ classical monocytes, $CD14^+/CD16^+$ intermediate monocytes, and $CD14^-/CD16^+$ nonclassical monocytes (Fig. 1A). We previously described the continuous differentiation from classical monocytes to intermediate and nonclassical monocytes (8), and in this study, focused on classical monocytes that directly traffic from bone marrow to blood. Additional markers for immune-phenotyping neutrophils, basophils, and classical monocytes in rhesus macaques are shown in Supplemental Fig. 1.

Neutrophils, basophils, and classical monocytes exhibit distinct kinetics in blood during homeostasis

At the time of BrdU administrations, dividing HSCs and granulocyte–monocyte progenitor cells in bone marrow will incorporate the BrdU as thymidine analog. Based on phenotyping and gating strategies shown in Fig. 1A, we measured the fraction of BrdU-labeled cells within each population and followed their movement into blood 1, 2, 4, 7, 10, and 14 d after BrdU administration. The length of time each cell type remains in the bone marrow differed. BrdU-labeled neutrophils began to be observed in blood 4 d post-BrdU, increased on day 5, reached the highest observed percentage on about day 7, and were cleared from blood by ~14 d post-BrdU (Fig. 2A, Supplemental Fig. 2A, 2B). Labeled basophils were first observed in blood 2 d post-BrdU, reached the highest observed percentage on day 4, and were cleared over the course of ~14 d (Fig. 2B, Supplemental Fig. 2A). BrdU-labeled classical monocytes appeared in blood as soon as 1 d later, reached the highest observed percentage 2 d post-BrdU, and were cleared by 8–10 d post-BrdU, as also reported previously by Sugimoto et al. (8) and shown in this study for comparison (Fig. 2C, Supplemental Fig. 2A). This suggested that basophil- and neutrophil-differentiating cells require at least 2 and 4 d, respectively, in bone marrow after division until trafficking to blood, whereas monocyte-differentiating cells enter the blood as early as 1 d after division. These results were consistent among the adult rhesus macaques examined and suggested that 1) BrdU-labeled cells could be readily detected and measured in blood following a single bolus injection of BrdU and 2) during homeostasis, neutrophils, basophils, and monocytes each exhibited consistently distinct kinetics of cell differentiation in bone marrow and trafficking to blood.

Mathematical kinetics modeling of blood half-life and daily production of myeloid cells

To estimate half-life and daily production of each myeloid cell population in the blood, we developed and applied a mathematical model to fit kinetics data from BrdU incorporation by neutrophils, basophils, and classical monocytes. Unincorporated BrdU is cleared in vivo within a short time (13, 14) and only progenitor cells

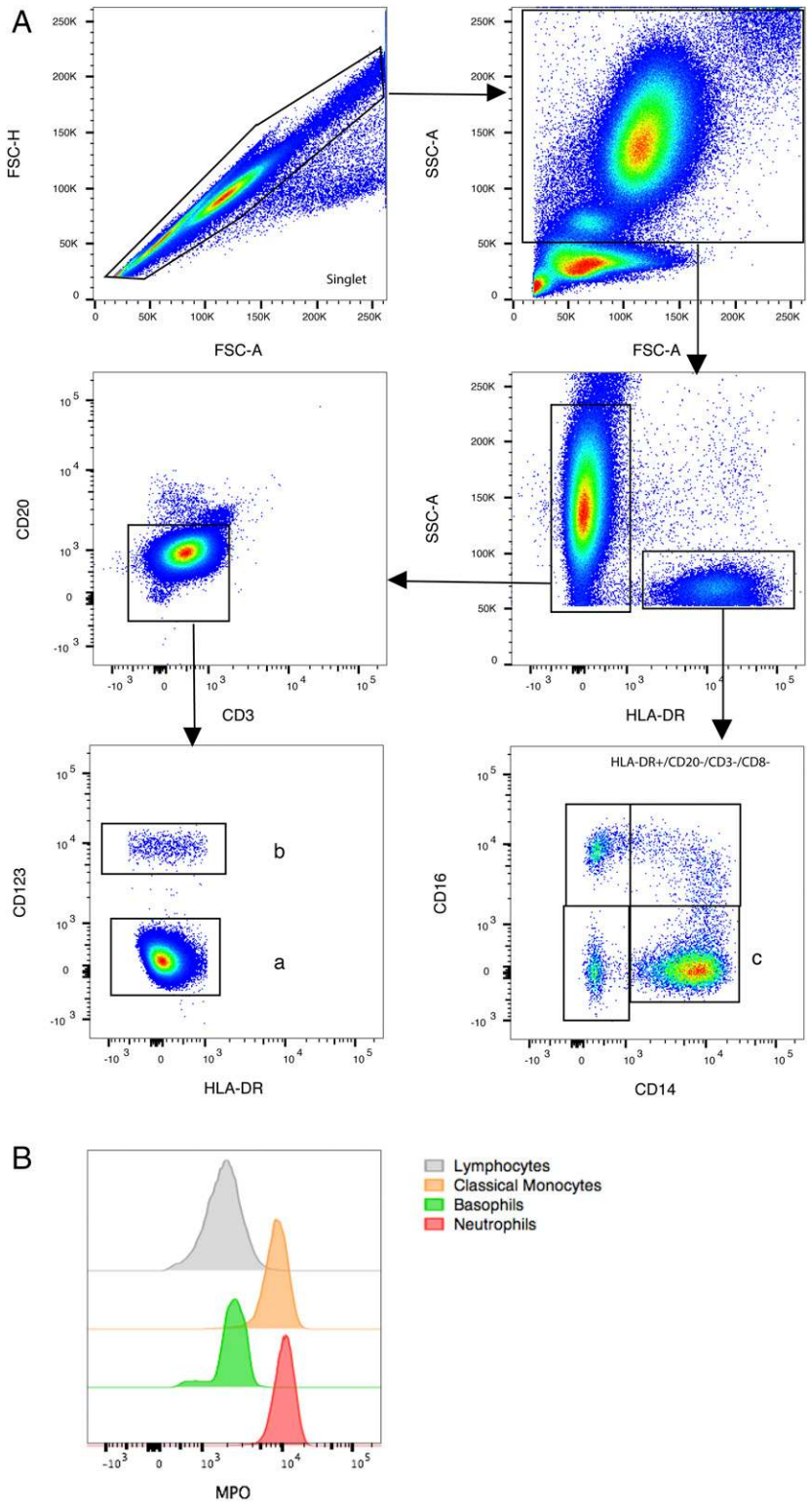

FIGURE 1. Phenotype analysis of neutrophils, basophils, and monocytes in peripheral blood of rhesus macaques. EDTA-treated blood samples were processed, stained with Abs (Table II), and analyzed by flow cytometry as described in the *Materials and Methods*. (**A**) The gating strategies of myeloid-lineage cells were indicated for (**a**) neutrophils = single cells, FSC/SSC$^{high/dim}$, HLA-DR$^-$, CD3$^-$, CD20$^-$, CD123$^-$; (**b**) basophils = single cells, FSC/SSC$^{high/dim}$, HLA-DR$^-$, CD123$^+$; and (**c**) classical monocytes = single cells, FSC/SSC^{dim}, HLA-DR$^+$, CD14$^+$CD16$^-$. (**B**) MPO expression was shown for neutrophils, basophils, classical monocytes, and lymphocytes gated from the above strategy.

proliferating within the first 1–2 h after administration incorporate detectable levels of BrdU. We fitted the data to Eq. 13, allowing M_0, k, and T to be free parameters. In the second group of animals that were 3 to 19 y old, we allowed M_0 and k to be free parameters and fixed T to the results from the first group of animals for improved calculations. Turnover rates (k values as described in the *Materials and Methods*) were calculated from the best-fit curves (Supplemental Fig. 2C) for the BrdU incorporation kinetics of 11 animals in group 1 (Fig. 3A). The results estimated the half-life of neutrophils as 1.63 ± 0.16 d, and the daily production as 1.42 ± 0.44 × 10^9 cells/l/d. Half-life and daily production of basophils were estimated as 1.78 ± 0.30 d and 5.89 × 10^6 cells/l/d, respectively. The half-life of classical monocytes was estimated at 1.01 ± 0.15 d with daily production as 3.09 ± 1.3 × 10^8 cells/l/d (Fig. 3B, 3C, Supplemental Table I). The half-lives for neutrophils and basophils were similar at ~1.6 and 1.7 d, respectively, that were slightly longer than the 1-d half-life of classical monocytes.

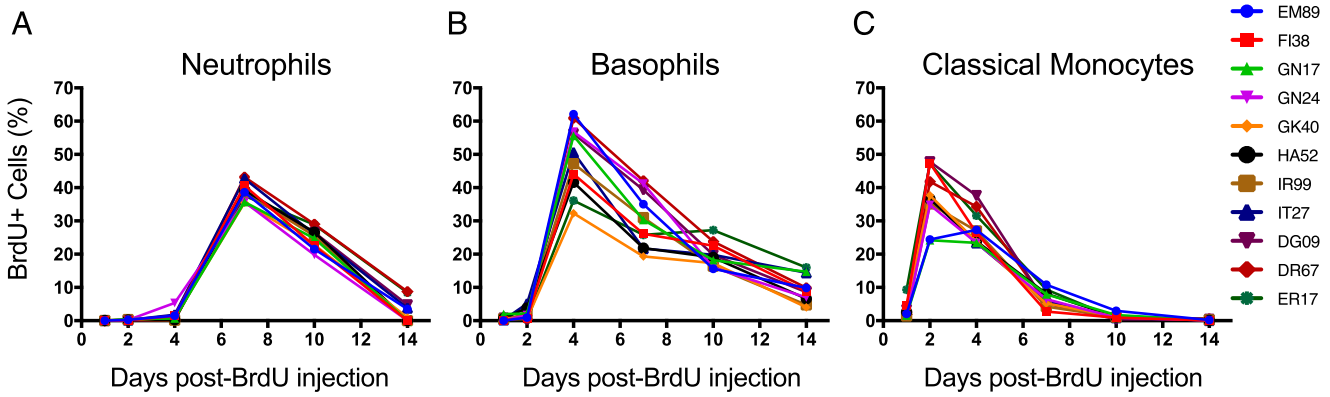

FIGURE 2. Neutrophils, basophils, and classical monocytes exhibit distinct kinetics in blood during homeostasis. Single-bolus BrdU (60 mg/kg body weight) was administrated i.v. to 11 rhesus macaques aged 5–10 y old (group 1; Table I) and EDTA-treated blood samples were collected 1, 2, 4, 7, and 14 d later for staining and flow cytometry analysis. Neutrophils (**A**), basophils (**B**), and classical monocytes (**C**) were gated based on the strategy described in Fig. 1A, and the percentages of BrdU-labeled cells were measured in each subset. Results from monocytes in (C) were previously published by Sugimoto et al. (8) and presented in this study for comparison with permission of the publisher.

BrdU kinetics of neutrophil- and basophil-differentiating progenitor cells in bone marrow

To further assess the kinetics and validate biological relevance of our mathematical model, we examined bone marrow aspirates collected 24 h and 4, 7, and 10 d post-BrdU administration from 8 of the 11 adult animals. Based on information from humans in which bone marrow neutrophil–differentiating cells started to express CD11b at the myelocyte stage and monocytes/macrophages express HLA-DR (17), neutrophil-differentiating cells in the rhesus macaque bone marrow were gated by singlet/CD45^{+}/FSC-SSC^{high}/CD3^{-}/CD20^{-}/CD11b^{+}/HLA-DR^{-} (Fig. 4A). This population appeared to mainly contain the postmitotic pool of neutrophils, and it was not the initial progenitor cells that incorporated BrdU because only a low percentage of these cells were labeled 24 h post-BrdU. In the bone marrow, the neutrophil-differentiating progenitor cells that incorporated BrdU reached the highest observed percentage levels on day 4 and then gradually decreased 7–10 d post-BrdU (Fig. 4B).

Basophil-differentiating cells in bone marrow were gated by singlet/FSC-SSC^{high}/CD3^{-}/CD20^{-}/CD123^{bright}/HLA-DR^{-} (Fig. 4C). Although, CD123 is expressed on other types of precursor cells in normal human bone marrow such as B cell precursors and common myeloid/granulocyte–macrophage progenitor cells (18), CD123 expression on basophils and basophil-differentiating cells is higher and at higher FSC/SSC (19, 20). The results also demonstrated that a higher percentage of basophil-committed progenitor cells in bone marrow were BrdU-labeled 1 d post-BrdU compared with the neutrophil-differentiating cells (Fig. 4B, 4D).

Chronological aging correlated with lower production of neutrophils and basophils and shorter half-life of classical monocytes

We showed that myeloid cells required constant replenishment from bone marrow hematopoiesis during homeostasis. In humans, the bone marrow cellularity declines with age (21), and the HSCs from the elderly have shown skewing toward myelopoiesis potential versus lymphopoiesis potential ex vivo (22). However, the effect of aging on the myeloid cell kinetics in vivo is still not clear. So, we examined this in a group of clinically healthy rhesus macaques of both sexes between 3 and 19 y of age (group 2; Table I). EDTA-blood was collected at 1, 4, 7, 10, and 14 d after single-bolus i.v. BrdU administration for immunostaining and flow cytometry as described in Fig. 1. Interestingly, granulocytes (neutrophils and basophils) and classical monocytes exhibited different patterns of kinetic changes with increasing age. The half-life of neutrophils and basophils remained similar at ~1.75 and 1.81 d, respectively, across all ages (Fig. 5A, 5B, 5D, 5E), whereas there was a significant negative correlation

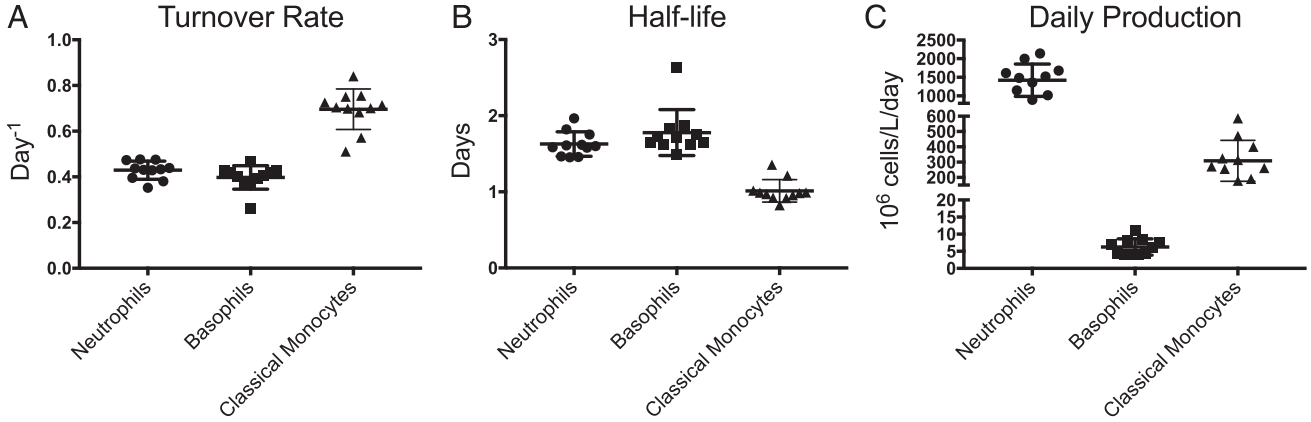

FIGURE 3. Rapid turnover of neutrophils, basophils and classical monocytes, and massive production of neutrophils in rhesus macaques during homeostasis. (**A**) Turnover rates for neutrophils, basophils, and classical monocytes (k values as described in *Materials and Methods*) were calculated from the best-fit curves to fit the mathematical model to the BrdU incorporation kinetics. (**B**) Half-life values for neutrophils, basophils, and classical monocytes were calculated as $ln(2)/k$. (**C**) Daily cell production numbers for neutrophils, basophils, and classical monocytes were calculated as absolute cell counts divided by the average circulating lifespans. Each data point represents results from one animal (n = 11). All results were expressed as the mean ± SD for each cell population.

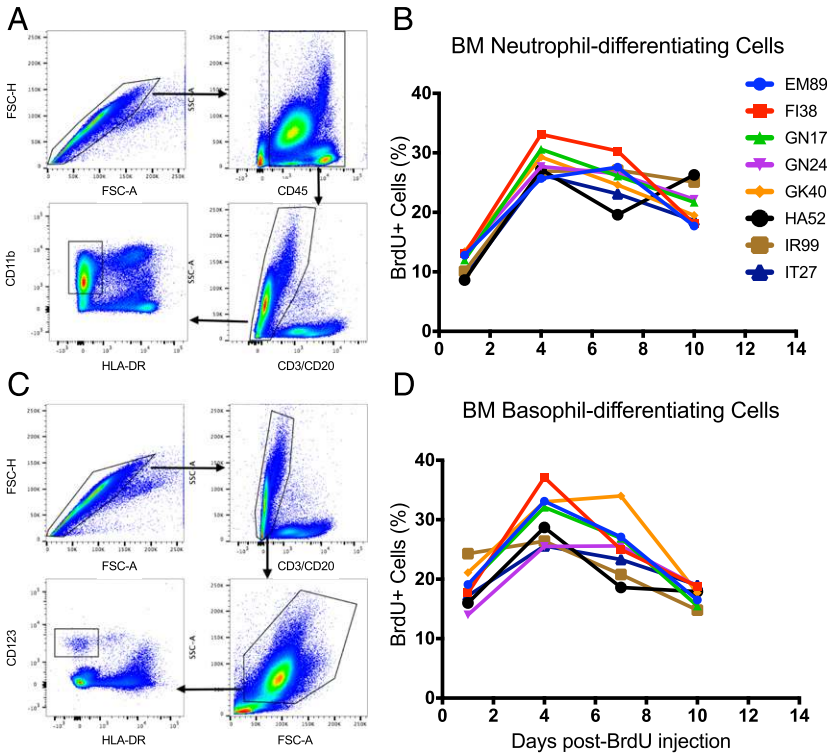

FIGURE 4. Gating strategy and BrdU kinetics of neutrophil- and basophil-differentiating progenitor cells in bone marrow (BM). BM aspirates were collected, stained, and analyzed 1, 4, 7, and 10 d after i.v. BrdU administration from 8 of the 11 animals assessed in Fig. 2. (**A**) Neutrophil-differentiating cells were gated as Singlet/CD45$^+$/FSC-SSC^{high}/CD3$^-$/CD20$^-$/CD11b$^+$/HLA-DR$^-$. (**C**) Basophil-differentiating cells were gated as singlet/ FSC-SSC^{high}/ CD3$^-$/CD20$^-$/CD123^{bright}/HLA-DR$^-$. The percentage of BrdU-labeled (**B**) neutrophil- and (**D**) basophil-differentiating cells in BM was low on day 1, increased on day 4, and then was declining by days 7–10.

between the numbers of neutrophils and basophils in blood and ages (Supplemental Fig. 3A, 3B). The similar half-life but lower number of neutrophils and basophils in blood calculated to a significant negative correlation between daily productions with age (Fig. 5G, 5H). In contrast, there was a significant negative correlation between half-lives of classical monocytes and age (Fig. 5C, 5F) as well as a significant negative correlation between absolute counts of classical monocytes in blood and age (Supplemental Fig. 3C). As a result, daily production of classical monocytes remained similar across all ages (Fig. 5I). Similar results were observed after comparing differences among animals divided into four age groups of 3–5 y old ($n = 4$), 5–10 y old ($n = 8$), 10–18 y old ($n = 10$), and >18 y old ($n = 11$) by Kruskal–Wallis test (Supplemental Fig. 3D–I), except that the change of basophil's daily productions among groups didn't reach statistical significance ($p = 0.076$).

Discussion

Conflicting results have been reported about the half-life of neutrophils (23–26) and monocytes (27) in humans, whereas such information is essentially absent about basophils (28, 29). In this study, we applied in vivo labeling with the thymidine analog, BrdU, to investigate myeloid-lineage cell development and kinetics in rhesus macaques that are more closely related genetically and physiologically to humans than are rodents and thereby provide a good model to better understand human myeloid cell kinetics. Furthermore, studies in humans are more limited by the use and administration route of labeling agents, as well as accessibility to repeated bone marrow, blood, and tissue sampling, than are rhesus macaques. We demonstrated relatively short half-lives of circulating neutrophils, basophils, and classical monocytes, and massive production of neutrophils and classical monocytes during homeostasis via BrdU in vivo labeling. Furthermore, the distinct kinetic patterns of neutrophils, basophils, and classical monocytes were internally consistent among the monkeys evaluated.

Neutrophils are the predominant myeloid and WBC component in blood of humans and nonhuman primates. The half-life of blood neutrophils in rhesus macaques was calculated at ~1.63 d compared with previous estimated circulating half-lives of neutrophils ranging between 7 h and 3.8 d in humans (23–26). The earlier studies on human neutrophil kinetics used adoptive transfer techniques and/or toxic radioactive labeling methods that likely altered the active state of neutrophils, resulting in an underestimated half-life of neutrophils (23). Two recent in vivo studies that used nontoxic labeling methods estimated the half-lives of circulating neutrophils in humans at 3.8 d and 19 h, respectively (24, 25). This discrepancy was considered by Lahoz-Beneytez et al. (25) to be due to their mathematical models rather than the labeling methods being used. Lahoz-Beneytez's model used an empirical parameter R representing the ratio of blood neutrophils to bone marrow mitotic neutrophil precursors; the estimation of R was based on several other studies that examined the maturation stage of neutrophil precursors in bone marrow by morphology rather than by direct labeling to assess cell division (25, 26, 30). The longer and slower uptake phase of the ^2H_2O and deuterium-labeled glucose uptake via drinking water in the Pillay et al. (24) and Lahoz-Beneytez et al. (25) studies, respectively, may also have influenced the neutrophil half-life estimations. Our calculated neutrophil half-life of 1.6 d in rhesus macaques was intermediate to the two values reported by the above two groups and was based on a single bolus i.v. labeling strategy that simplified the label uptake phase calculations.

We also examined the differentiation phase of neutrophils after proliferation in bone marrow. BrdU incorporation occurs prior to expression of the CD11b$^+$HLA-DR$^-$ phenotype in neutrophil precursors in bone marrow, and this CD11b$^+$/HLA-DR$^-$ subset in bone marrow exhibited low levels of BrdU incorporation 1 d after BrdU injection with increasing levels observed on day 4, followed by gradual declines on days 7 and 10. The estimated daily production of neutrophils at 1.42 ± 0.44 × 10^9 cells/l/d in rhesus macaques was lower than the previously reported 0.87 × 10^9 cells/kg body weight per day in

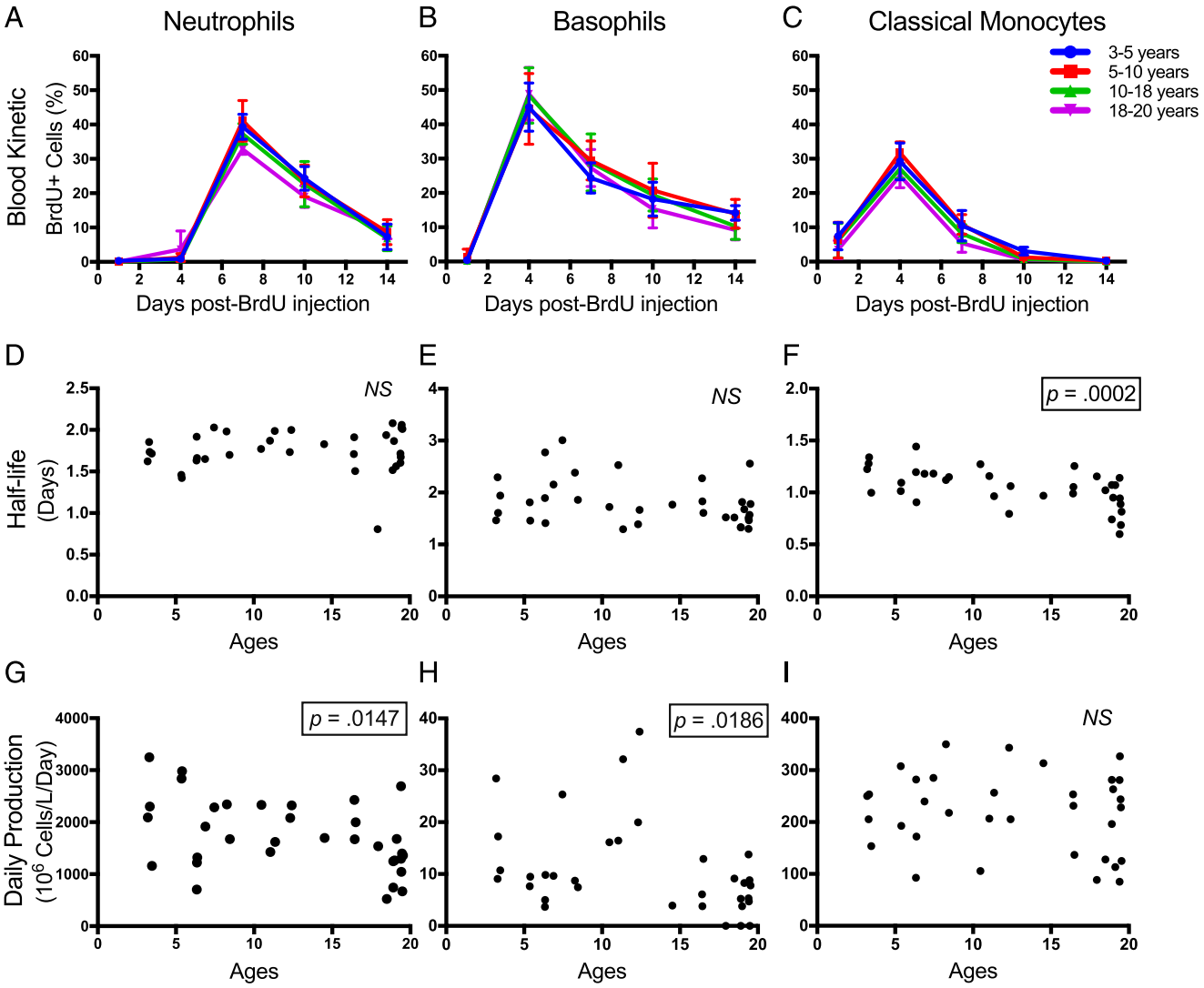

FIGURE 5. Chronological aging correlated with lower production of neutrophils and basophils and a shorter half-life of classical monocytes. EDTA-treated blood samples from rhesus macaques were collected and stained (group 2; Table I) 1, 4, 7, 10, and 14 d after i.v. BrdU administration. The $BrdU^+$ cell fraction, half-life, and daily production were measured and calculated, respectively, for neutrophils (**A**, **D**, and **G**), basophils (**B**, **E**, and **H**), and classical monocytes (**C**, **F**, and **I**). Blood kinetics were expressed as the mean ± SD of the $BrdU^+$ cell fraction for each age group. Nonparametric Spearman correlation tests were used to compare half-life and daily production of cell types against age of the animals. $p < 0.05$ was considered statistically significant.

humans (or 11.98×10^9 cells cells/l/d based on 5.3 l blood in a 73 kg man) that was likely based on the longer estimation of neutrophil half-life at 1.63 d in our study compared with 7 h estimated by Dancey et al. (26). Calculation for neutrophil bone marrow transit of 4–5 d in rhesus macaques was similar to the 5–6 d reported for humans (24–26).

Our results also suggested that neutrophils subsequently traffic to tissues after circulating in blood. For example, BrdU-labeled neutrophils were detected in lung biopsies 7 d after BrdU injection of rhesus macaques (data not shown). In addition, the fraction of BrdU-labeled neutrophils in the bone marrow remained at ~20%, which is higher than we originally expected, and this could have resulted from homing of the aged neutrophils back to bone marrow for clearance (31, 32).

Like neutrophils, monocytes contribute to the innate immune system and in rhesus macaques, differentiate from $CD14^+/CD16^-$ classical monocytes to $CD14^+/CD16^+$ intermediate monocytes and to $CD14^-/CD16^+$ nonclassical monocytes in blood (8). Thus, earlier estimates of monocyte half-life (27) probably represented the average monocyte half-life rather than the kinetics of specific monocyte subpopulations. We calculated the half-life of classical monocytes in blood at just over 1 d in adult macaques that were produced at a rate of $\sim 3 \times 10^8$ cells/l/d during homeostasis. The transit time of monocytes in the bone marrow after proliferation is <1 d, which is much shorter than for neutrophils and basophils. Classical monocytes were predominant over intermediate and nonclassical monocytes and appeared to leave blood circulation to transition into tissue macrophages, consistent with two recent reports on humans (33, 34). In our earlier studies (35), BrdU-labeled monocytes that trafficked into interstitial lung tissues of rhesus macaques were relatively shorter-lived. Conversely, alveolar lung macrophages that had not incorporated BrdU within the 7–10 d time course were considered longer-lived. Thus, in vivo BrdU labeling studies can be applied for examining monocyte and tissue macrophage subpopulation kinetics that influence immune responses.

Less is known about the kinetics of basophils, mainly due to their paucity in blood. Ohnmacht et al. (36) used BrdU labeling in mice and estimated the lifespan of basophils from blood to tissues at

60 h based on the assumption that the labeled basophils enter tissues at a constant rate and independent of the concentration of cells. To our knowledge, the current study is the first to demonstrate that basophils exhibit distinct kinetics and shorter bone marrow transit time compared with neutrophils in nonhuman primates. Surprisingly, basophils also have a relatively short half-life in blood at ∼1.7 d (slightly longer than neutrophils) and are replenished from bone marrow at a rate of 5.89×10^6 cells/l/d during homeostasis. BrdU incorporation into the $CD123^+HLA\text{-}DR^-$ basophil-differentiating cell subset in bone marrow was higher 1 d post-BrdU than for neutrophil-differentiating cells, and the decay 4 d after BrdU injection was also faster to coincide with basophil kinetics in peripheral blood. Although we were limited from collecting bone marrow samples at daily intervals between 1 and 4 d after BrdU injection, the results suggested that peak BrdU labeling of basophils in bone marrow occurred within this timeframe.

We calculated the daily production of the different myeloid cells described above based on their average circulating lifespan and absolute count in blood circulation as well as on the assumption that each gated cell population is homogenous in the blood. That is to say, it is still possible that small fractions of cells exist in the above cell populations that have a much slower kinetics or recirculate back from tissue to blood. Such subsets, if they exist, are considered to comprise small fractions of the whole, given that we didn't observe any consistent BrdU labeling in the above populations long-term after label injection (data not shown).

The initial myeloid cell BrdU kinetics were evaluated in rhesus macaques between 5 and 10 y of age that are considered young adults equivalent to humans of ∼18–40 y of age (or 3.5–4 times older than rhesus macaques). A set of rhesus macaques aged 3–19 y of age (∼10–75 y of age in humans) of both sexes were then evaluated to examine effects of chronological aging on myeloid cell kinetics. Elderly people and animals are more susceptible to infections (37), and HSCs in bone marrow from the elderly exhibit a trend for less regenerative potential compared with HSCs from younger adults (22). This might partially be reflected by the slight decrease of innate immune cell numbers observed in elderly humans (37–39) as well as in rhesus macaques (40). Absolute cell numbers, however, do not reflect the movement or the production of the cells. Throughout the age range of 3–19 y in the rhesus macaques, neutrophil production declined in daily output, whereas neutrophil half-life remained unchanged. Interestingly, daily production of classical monocytes remained unchanged, whereas the half-life of monocytes declined with increasing age. These may reflect different mechanisms for neutrophils and monocytes to compensate for limited bone marrow hematopoiesis or output as animals age. We didn't observe significant differences in kinetics, half-life, or daily production in all three cell types between age-matched male and female animals between 3 and 18 y of age in our study (data not shown). However, the combined effect of age and sex is still not clear because the animals >18 y old were all females in our study based on availability. Thus, it is important to investigate the potential sex effects, especially in the context of aging in future studies.

Overall, these results demonstrated the massive production of neutrophils and monocytes in bone marrow and rapid turnover of neutrophils, basophils, and classical monocytes in blood of rhesus macaques during homeostasis. Also, the rapid turnover rates of neutrophils, basophils, and classical monocytes were maintained in the older animals, albeit with a decrease of neutrophil production with aging. Consistency observed between animals suggested a tight regulation of the half-life and massive production that may be required to maintain homeostasis.

Acknowledgments

We thank Toni P. Penny, Edith M. Walker, Erin M. Haupt, Nadia Slisarenko, Jeanne M. Perkins, Kelly A. Goff, Julie A. Bruhn, and Calvin R. Lanclos in the Division of Immunology, Robert Blair in the Division of Comparative Pathology, and Jason P. Dufour in the Division of Veterinary Medicine at Tulane National Primate Research Center for their assistance.

Disclosures

The authors have no financial conflicts of interest.

References

1. Kolaczkowska, E., and P. Kubes. 2013. Neutrophil recruitment and function in health and inflammation. *Nat. Rev. Immunol.* 13: 159–175.
2. Shi, C., and E. G. Pamer. 2011. Monocyte recruitment during infection and inflammation. *Nat. Rev. Immunol.* 11: 762–774.
3. Summers, C., S. M. Rankin, A. M. Condliffe, N. Singh, A. M. Peters, and E. R. Chilvers. 2010. Neutrophil kinetics in health and disease. *Trends Immunol.* 31: 318–324.
4. Geering, B., C. Stoeckle, S. Conus, and H.-U. Simon. 2013. Living and dying for inflammation: neutrophils, eosinophils, basophils. *Trends Immunol.* 34: 398–409.
5. Siracusa, M. C., B. S. Kim, J. M. Spergel, and D. Artis. 2013. Basophils and allergic inflammation. *J. Allergy Clin. Immunol.* 132: 789–801.
6. Voehringer, D. 2009. The role of basophils in helminth infection. *Trends Parasitol.* 25: 551–556.
7. Ziegler-Heitbrock, L., P. Ancuta, S. Crowe, M. Dalod, V. Grau, D. N. Hart, P. J. M. Leenen, Y.-J. Liu, G. MacPherson, G. J. Randolph, et al. 2010. Nomenclature of monocytes and dendritic cells in blood. *Blood* 116: e74–e80.
8. Sugimoto, C., A. Hasegawa, Y. Saito, Y. Fukuyo, K. B. Chiu, Y. Cai, M. W. Breed, K. Mori, C. J. Roy, A. A. Lackner, et al. 2015. Differentiation kinetics of blood monocytes and dendritic cells in macaques: insights to understanding human myeloid cell development. *J. Immunol.* 195: 1774–1781.
9. Doeing, D. C., J. L. Borowicz, and E. T. Crockett. 2003. Gender dimorphism in differential peripheral blood leukocyte counts in mice using cardiac, tail, foot, and saphenous vein puncture methods. *BMC Clin. Pathol.* 3: 3.
10. Mestas, J., and C. C. W. Hughes. 2004. Of mice and not men: differences between mouse and human immunology. *J. Immunol.* 172: 2731–2738.
11. Institute for Laboratory Animal Research. 2011. *Guide for the Care and Use of Laboratory Animals.* National Academies Press, Washington, D.C.
12. Hasegawa, A., H. Liu, B. Ling, J. T. Borda, X. Alvarez, C. Sugimoto, H. Vinet-Oliphant, W.-K. Kim, K. C. Williams, R. M. Ribeiro, et al. 2009. The level of monocyte turnover predicts disease progression in the macaque model of AIDS. *Blood* 114: 2917–2925.
13. Kriss, J. P., Y. Maruyama, L. A. Tung, S. B. Bond, and L. Revesz. 1963. The fate of 5-bromodeoxyuridine, 5-bromodeoxycytidine, and 5-iododeoxycytidine in man. *Cancer Res.* 23: 260–268.
14. Matiašová, A., J. Sevc, J. Mikeš, R. Jendželovský, Z. Daxnerová, and P. Fedoročko. 2014. Flow cytometric determination of 5-bromo-2′-deoxyuridine pharmacokinetics in blood serum after intraperitoneal administration to rats and mice. *Histochem. Cell Biol.* 142: 703–712.
15. Oliphant, T. E. 2007. Python for scientific computing. *Comput. Sci. Eng.* 9: 10–20.
16. Sharma, M., P. Hegde, V. Aimanianda, R. Beau, M. S. Maddur, H. Sénéchal, P. Poncet, J.-P. Latgé, S. V. Kaveri, and J. Bayry. 2013. Circulating human basophils lack the features of professional antigen presenting cells. [Published erratum appears in 2013 *Sci. Rep.*10: 1038.] *Sci. Rep.* 3: 1188.
17. Terstappen, L. W., M. Safford, and M. R. Loken. 1990. Flow cytometric analysis of human bone marrow. III. Neutrophil maturation. *Leukemia* 4: 657–663.
18. Hassanein, N. M., F. Alcancia, K. R. Perkinson, P. J. Buckley, and A. S. Lagoo. 2009. Distinct expression patterns of CD123 and CD34 on normal bone marrow B-cell precursors ("hematogones") and B lymphoblastic leukemia blasts. *Am. J. Clin. Pathol.* 132: 573–580.
19. Toba, K., T. Koike, A. Shibata, S. Hashimoto, M. Takahashi, M. Masuko, T. Azegami, H. Takahashi, and Y. Aizawa. 1999. Novel technique for the direct flow cytofluorometric analysis of human basophils in unseparated blood and bone marrow, and the characterization of phenotype and peroxidase of human basophils. *Cytometry* 35: 249–259.
20. Han, X., J. L. Jorgensen, A. Brahmandam, E. Schlette, Y. O. Huh, Y. Shi, S. Awagu, and W. Chen. 2008. Immunophenotypic study of basophils by multiparameter flow cytometry. *Arch. Pathol. Lab. Med.* 132: 813–819.
21. Ogawa, T., M. Kitagawa, and K. Hirokawa. 2000. Age-related changes of human bone marrow: a histometric estimation of proliferative cells, apoptotic cells, T cells, B cells and macrophages. *Mech. Ageing Dev.* 117: 57–68.
22. Pang, W. W., E. A. Price, D. Sahoo, I. Beerman, W. J. Maloney, D. J. Rossi, S. L. Schrier, and I. L. Weissman. 2011. Human bone marrow hematopoietic stem cells are increased in frequency and myeloid-biased with age. *Proc. Natl. Acad. Sci. USA* 108: 20012–20017.
23. Tak, T., K. Tesselaar, J. Pillay, J. A. Borghans, and L. Koenderman. 2013. What's your age again? Determination of human neutrophil half-lives revisited. *J. Leukoc. Biol.* 94: 595–601.
24. Pillay, J., I. den Braber, N. Vrisekoop, L. M. Kwast, R. J. de Boer, J. A. M. Borghans, K. Tesselaar, and L. Koenderman. 2010. In vivo labeling with 2H2O reveals a human neutrophil lifespan of 5.4 days. *Blood* 116: 625–627.

25. Lahoz-Beneytez, J., M. Elemans, Y. Zhang, R. Ahmed, A. Salam, M. Block, C. Niederalt, B. Asquith, and D. Macallan. 2016. Human neutrophil kinetics: modeling of stable isotope labeling data supports short blood neutrophil half-lives. *Blood* 127: 3431–3438.
26. Dancey, J. T., K. A. Deubelbeiss, L. A. Harker, and C. A. Finch. 1976. Neutrophil kinetics in man. *J. Clin. Invest.* 58: 705–715.
27. Whitelaw, D. M. 1972. Observations on human monocyte kinetics after pulse labeling. *Cell Tissue Kinet.* 5: 311–317.
28. Siracusa, M. C., J. G. Perrigoue, M. R. Comeau, and D. Artis. 2010. New paradigms in basophil development, regulation and function. *Immunol. Cell Biol.* 88: 275–284.
29. Min, B., M. A. Brown, and G. Legros. 2012. Understanding the roles of basophils: breaking dawn. *Immunology* 135: 192–197.
30. Harrison, W. J. 1962. The total cellularity of the bone marrow in man. *J. Clin. Pathol.* 15: 254–259.
31. Furze, R. C., and S. M. Rankin. 2008. The role of the bone marrow in neutrophil clearance under homeostatic conditions in the mouse. *FASEB J.* 22: 3111–3119.
32. Casanova-Acebes, M., C. Pitaval, L. A. Weiss, C. Nombela-Arrieta, R. Chèvre, N. A-González, Y. Kunisaki, D. Zhang, N. van Rooijen, L. E. Silberstein, et al. 2013. Rhythmic modulation of the hematopoietic niche through neutrophil clearance. *Cell* 153: 1025–1035.
33. Patel, A. A., Y. Zhang, J. N. Fullerton, L. Boelen, A. Rongvaux, A. A. Maini, V. Bigley, R. A. Flavell, D. W. Gilroy, B. Asquith, et al. 2017. The fate and lifespan of human monocyte subsets in steady state and systemic inflammation. *J. Exp. Med.* 214: 1913–1923.
34. Tak, T., J. Drylewicz, L. Conemans, R. J. de Boer, L. Koenderman, J. A. M. Borghans, and K. Tesselaar. 2017. Circulatory and maturation kinetics of human monocyte subsets in vivo. *Blood* 130: 1474–1477.
35. Cai, Y., C. Sugimoto, M. Arainga, X. Alvarez, E. S. Didier, and M. J. Kuroda. 2014. In vivo characterization of alveolar and interstitial lung macrophages in rhesus macaques: implications for understanding lung disease in humans. *J. Immunol.* 192: 2821–2829.
36. Ohnmacht, C., and D. Voehringer. 2009. Basophil effector function and homeostasis during helminth infection. *Blood* 113: 2816–2825.
37. Shaw, A. C., D. R. Goldstein, and R. R. Montgomery. 2013. Age-dependent dysregulation of innate immunity. *Nat. Rev. Immunol.* 13: 875–887.
38. De Martinis, M., M. Modesti, and L. Ginaldi. 2004. Phenotypic and functional changes of circulating monocytes and polymorphonuclear leucocytes from elderly persons. *Immunol. Cell Biol.* 82: 415–420.
39. Seidler, S., H. W. Zimmermann, M. Bartneck, C. Trautwein, and F. Tacke. 2010. Age-dependent alterations of monocyte subsets and monocyte-related chemokine pathways in healthy adults. *BMC Immunol.* 11: 30.
40. Didier, E. S., C. Sugimoto, L. C. Bowers, I. A. Khan, and M. J. Kuroda. 2012. Immune correlates of aging in outdoor-housed captive rhesus macaques (*Macaca mulatta*). *Immun. Ageing* 9: 25.